NJC

Single Particle ICP-MS and GC-MS Provide New Insight into the Forming Mechanisms for AgNPs Green Synthesis

Journal:	*New Journal of Chemistry*
Manuscript ID	NJ-ART-12-2018-006291.R1
Article Type:	Paper
Date Submitted by the Author:	22-Jan-2019
Complete List of Authors:	Zhang, Huiling; Nanjing University, School of Environment HUANG, Yuxiong; University of California, Santa Barbara, Bren School of Environmental Science and Management Gu, Jianqiang; Nanjing University, School of Environment Keller, Arturo; University of California, Santa Barbara, Bren School of Environmental Science and Management Qin, Yuwei; University of California Santa Barbara, Bren School of Environmental Science & Management Bian, Yue; Nanjing University, School of electronic science and engineering Tang, Kun; Nanjing University, Electronic Sci & Eng Qu, Xiaolei; Nanjing University, School of the Environment Ji, Rong; Nanjing University, School of the Environment Zhao, Lijuan; Nanjing University, Environmental Science

Single Particle ICP-MS and GC-MS Provide New Insight into the Forming Mechanisms for AgNPs Green Synthesis

Huiling Zhang,[a,1] Yuxiong Huang,[b,c,1] Jianqiang Gu,[a] Arturo Keller,[b] Yuwei Qin,[b] Yue Bian,[d] Kun Tang,[d] Xiaolei Qu,[a] Rong Ji,[a*] Lijuan Zhao[a*]

[a] State Key Laboratory of Pollution Control and Resource Reuse, School of Environment, Nanjing University, Nanjing 210023, China

[b] Bren School of Environmental Science & Management, University of California, Santa Barbara, California 93106-5131, United States

[c] Shenzhen Environmental Science and New Energy Technology Engineering Laboratory, Tsinghua-Berkeley Shenzhen Institute, Shenzhen 518055, P. R. China.

[d] School of Electronic Science and Engineering, Nanjing University, Nanjing 210023, China

[1]H. Z. and Y. H. contributed equally to this manuscript, considered as co-first authors.

**Corresponding author*. Tel: +86 025-8968 0581; fax: +86 025-8968 0581.

Email address: ji@nju.edu.cn, ljzhao@nju.edu.cn

ABSTRACT

Green synthesis of metallic nanoparticles (NPs) using plant extracts has received considerable attention due to its environmentally and economically friendly nature. Various metabolites in plants such as amino acids, organic acids, sugars, phenolics have been speculated to be responsible for the synthesis of metallic NPs in previous studies. However, to date，there has been a lack of direct evidence linking specific metabolites to the reduction of metal ions to form metallic NPs. Here, AgNPs were synthesized using cucumber leaf extract and characterized by UV-visible spectroscopy, dynamic light scattering (DLS) and transmission electron spectroscopy (TEM). Single particle-inductively coupled plasma mass spectrometry (sp-ICP-MS) was used to investigate the size of newly synthesized NPs as well as the kinetics of particles forming. Gas chromatography-mass spectrometry (GC-MS) based metabolomics identified and quantified 245 metabolites in cucumber leaf extracts. By comparing the concentrations of metabolites before and after the reaction, the metabolites responsible for the synthesis were screened out. Reducing sugars (cellobiose, ribulose-5-phosphate, melibiose, 2-deoxy-D-glucose, tagatose, fructose, ribose, 3,6-anhydro-D-galactose) were markedly decreased after the reaction, indicating reducing sugar are involved in the biosynthesis process and possibly function as reducing agents. The key thermodynamic data of the reaction between Ag^+ and reducing sugar were obtained by using isothermal titration calorimetry (ITC), which further confirmed the interaction between Ag^+ and metabolites.

This study provides a deep insight into the reaction process and mechanism of green synthesized AgNPs.

KEYWORDS: Green synthesis; plant extracts; silver nanoparticle; single particle ICP-MS; ITC; metabolomics.

INTRODUCTION

Green synthesis of nanoparticles (NPs) has become a promising field of research in recent years. Plant-mediated biosynthesis of metallic nanoparticles is comparatively cost-effective and environmental-friendly compared to chemical methods.[1] There are many studies employing different plant extracts to mediate biosynthesis of various metal or metal oxide NPs[2-12]. However, current knowledge of key metabolites involved in the biosynthesis and the mechanisms of nanoparticles formation is quite poor.[13] Understanding the actual mechanisms underlying nanoparticle formation is necessary to develop a rational approach to control the size, shape, and crystallinity of the NPs.[13]

Plants generate a large number of primary metabolites such as organic acids, sugars, and amino acids; as well as numerous secondary metabolites which play an important role in defense and antioxidant, such as phenolic compounds, ascorbic acid, quinones, flavonoids, terpenoids, and polysaccharides. Among them, reducing sugars, proteins, and polyphenols have been postulated to act as reducing and stabilizing agents for synthesis of metal and metal oxide NPs in previous reports.[3, 14-16] Beattie and Haverkamp[17] found that chloroplasts, a subcellular organelle that produces abundant amounts of reducing sugars (i.e. glucose and fructose), accumulated the highest amounts of Silver nanoparticles (AgNPs) and thus they speculated that reducing sugars are likely responsible for the reduction of Ag^+ to Ag. Some studies[14, 18] showed that polysaccharides, proteins, flavonoids, and terpenoids, which

together promote the total reducing capacity of plant cells, could be involved in the biosynthesis of metal NPs and their stabilization. Kahrilas et al.[19] determined the metabolites in orange peel extract and assumed that aldehyde-containing and other reducing compounds participated in the generation of AgNPs. Begum et al.[20] proposed that polyphenols or flavonoids present in tea leaves were responsible for the AgNPs synthesis. This conclusion was reached since no AgNP was observed in leaf extract lacking polyphenols/flavonoids.

However, most of the proposed mechanism was just reasonable hypotheses, lacking direct experimental evidence.[13] In order to elucidate the underlying mechanism, metabolites must be precisely quantified before and after the reaction. Metabolomics was originally used to study the metabolic response of organisms to their environment. By using gas chromatograph-quadrupole time-of-flight mass spectrometer (GC-QTOF-MS) based metabolomics, we were able to identify and semi-quantify the relative level of hundreds of metabolites simultaneous in cucumber leaves and cucumber root exudate.[21, 22] We hypothesized that metabolomics can provide important screening information to identify and semi-quantitative analyze the metabolites that are involved in the AgNP biosynthesis process.

Base on the metabolomic screening data, we propose to further obtain the key thermodynamic data by using the isothermal titration calorimetry (ITC), which can directly measure the heat absorbed or released during the interaction to determine the changes in enthalpy ΔH, entropy ΔS, and Gibbs free energy ΔG of the adsorption process, as well as the affinity binding constant K_d and the interaction reaction stoichiometry.[23] Combining

these two novel approaches, the mechanism of AgNPs green synthesis would be revealed at the molecular level.

Cucumber leaves are agricultural by-products and have high levels of reducing metabolites.[24, 25] In this study, cucumber leaf extract was prepared and used as a reducing and stabilizing agent for AgNPs biosynthesis. After the AgNP synthesis condition was optimized and AgNPs were synthesized, the physicochemical properties of the obtained NPs were characterized by UV-vis spectrophotometry, dynamic light scattering (DLS) and transmission electron spectroscopy (TEM) and single particle-inductively coupled plasma mass spectrometry (sp-ICP-MS). In addition, GC-MS was employed to determine the content of metabolites before and after the reaction, by which, the role of specific reducing agents can be elucidated. The key thermodynamic data of the interaction between Ag^+ and cucumber leaf exacts were determined via ITC measurement. Finally, the antioxidant capacity of the AgNPs was evaluated.

MATERIALS AND METHOD

Preparation of Cucumber Leaf Extract. Cucumber seeds (Zhongnong No.28 F1) were purchased from Hezhiyuan Seed Corporation (Shandong, China). Before use, the seeds were treated with 5% NaClO for 30 min. After completely rinsing, the seeds were germinated in quartz sand in the dark at 25 °C for 7 days. After germination, the plants were transferred to Hoagland nutrient solution and cultivated for 5 weeks to generate sufficient biomass. The nutrient solution was replaced once per week. The cucumber leaves were harvested when the cucumber plants were 5 weeks old. Fresh cucumber leaves were collected and washed with DI water and oven-dried at 105 °C for 30 min followed by 70°C

for 8 hours. To prepare the leaf extract, 10 grams of oven-dried leaves powder were added to 100 mL of DI water and the mixture was boiled at 100 °C for 15 min. After cooling down, the solution was centrifuged at 10000 rpm for 10 min and the supernatant was collected and stored at 4 °C.

Chemicals. DI water was used for all the experiments. Silver nitrate ($AgNO_3$; Shanghai Reagent Company; ≥99.8%), ammonium hydroxide (NH_4OH; Aladdin industrial corporation (Shanghai, China); 25-28%); hydrochloric acid (HCl; 36-38%) and sodium hydroxide (NaOH; ≥96%) (Sinopharm chemical reagent Co., Ltd (Shanghai, China), were used in this study without further purification.

All chemicals and solvents for GC-MS analysis were analytical or HPLC grade. Water, methanol, pyridine, n-hexane, methoxylamine hydrochloride (97%), BSTFA with 1% TMCS were purchased from CNW Technologies GmbH (Düsseldorf, Germany). Trichloromethane was from Sinopharm Chemical Reagent Co., Ltd. (Shanghai, China). L-2-chlorophenylalanine was from Shanghai Hengchuang Bio-technology Co., Ltd. (Shanghai, China).

Biosynthesis of Silver NPs using Cucumber Leaf Extracts. An initial screening trial using UV-vis was performed to optimize AgNPs synthesis conditions, including pH, reaction temperature, reaction time and the ratio of $AgNO_3$ and leaf extracts (**Table S2-S3; Figure S1 and S2**). The formation of AgNPs was confirmed by measuring using UV-vis at 414 nm and color changes. UV-vis spectroscopic analyses of AgNPs were carried out as a function of reaction time and temperature using a Microplate Reader (Synergy H4 Hybrid Reader, Biotek, America) at a resolution of 2 nm. According to the preliminary assays, $AgNO_3$ at a concentration of 10 mM, leaf extract and $AgNO_3$ at a volume ratio of 1:1, pH

10.0, reaction time 4 h, and a reaction temperature of 80 °C were the optimal conditions to synthesize AgNPs (**Figure S3**).

Table S2. Trials to screen optimal reaction pH, temperature, time for synthesis of AgNP.

Number	pH	Temperature/°C	Time/h
1	4.02	25	0.5
2	4.02	25	1
3	4.02	25	2
4	4.02	25	4
5	4.02	50	0.5
6	4.02	50	1
7	4.02	50	2
8	4.02	50	4
9	4.02	80	0.5
10	4.02	80	1
11	4.02	80	2
12	4.02	80	4
13	5.86	25	0.5
14	5.86	25	1
15	5.86	25	2
16	5.86	25	4
17	5.86	50	0.5
18	5.86	50	1
19	5.86	50	2
20	5.86	50	4
21	5.86	80	0.5
22	5.86	80	1
23	5.86	80	2
24	5.86	80	4
25	10.01	25	0.5
26	10.01	25	1
27	10.01	25	2
28	10.01	25	4
29	10.01	50	0.5
30	10.01	50	1
31	10.01	50	2
32	10.01	50	4
33	10.01	80	0.5
34	10.01	80	1

35	10.01	80	2
36	10.01	80	4

Table S3. Trials to screen optimal ratio of $AgNO_3$ and leaf extract for green synthesis of AgNP.

Number	pH	Temperature/°C	Time/h	Ag/leaf extracts
1	10.02	80	0.5	1:4
2	10.02	80	1	1:4
3	10.02	80	2	1:4
4	10.02	80	4	1:4
5	10.02	80	0.5	1:1
6	10.02	80	1	1:1
7	10.02	80	2	1:1
8	10.02	80	4	1:1
9	10.02	80	0.5	2:1
10	10.02	80	1	2:1
11	10.02	80	2	2:1
12	10.02	80	4	2:1
13	10.02	80	0.5	4:1
14	10.02	80	1	4:1
15	10.02	80	2	4:1
16	10.02	80	4	4:1

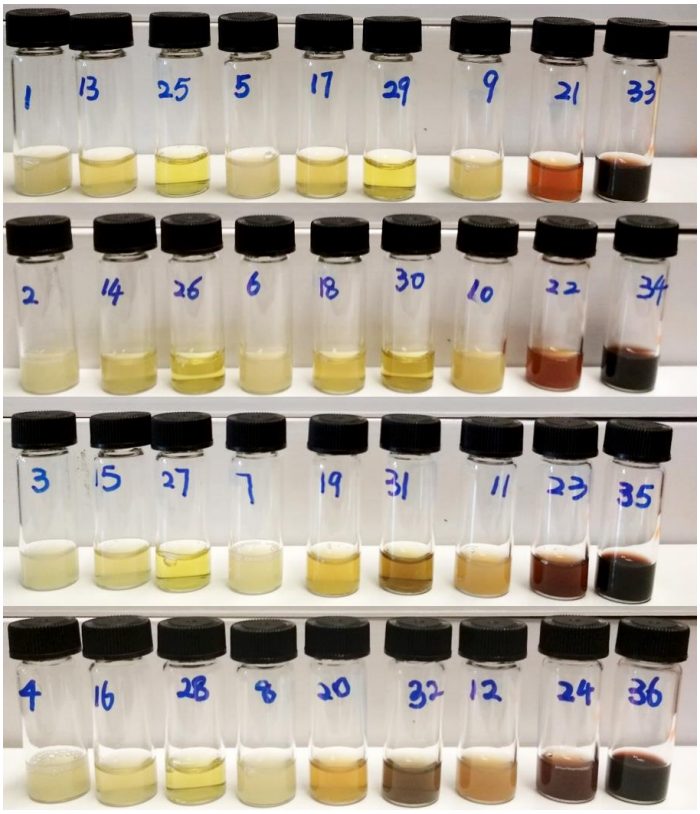

Figure S1. The color change of the Ag^+ solution for optimal green synthesis screening. Trials number with detailed reaction pH, temperature, time were listed in Table S2.

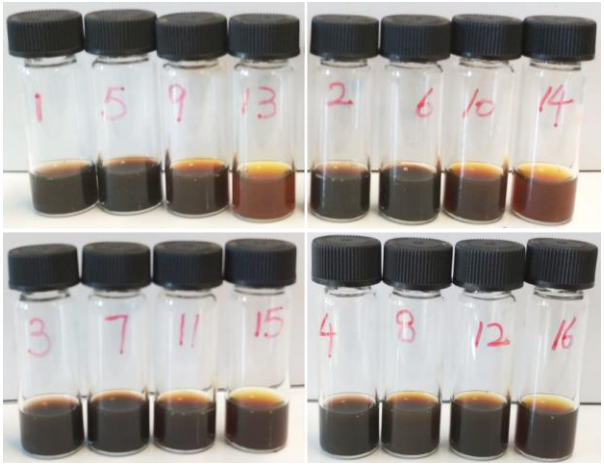

Figure S2. The color change of the Ag^+ solution for optimal green synthesis screening. Trials number with the detailed ratio of $AgNO_3$ to leaf were listed in Table S3.

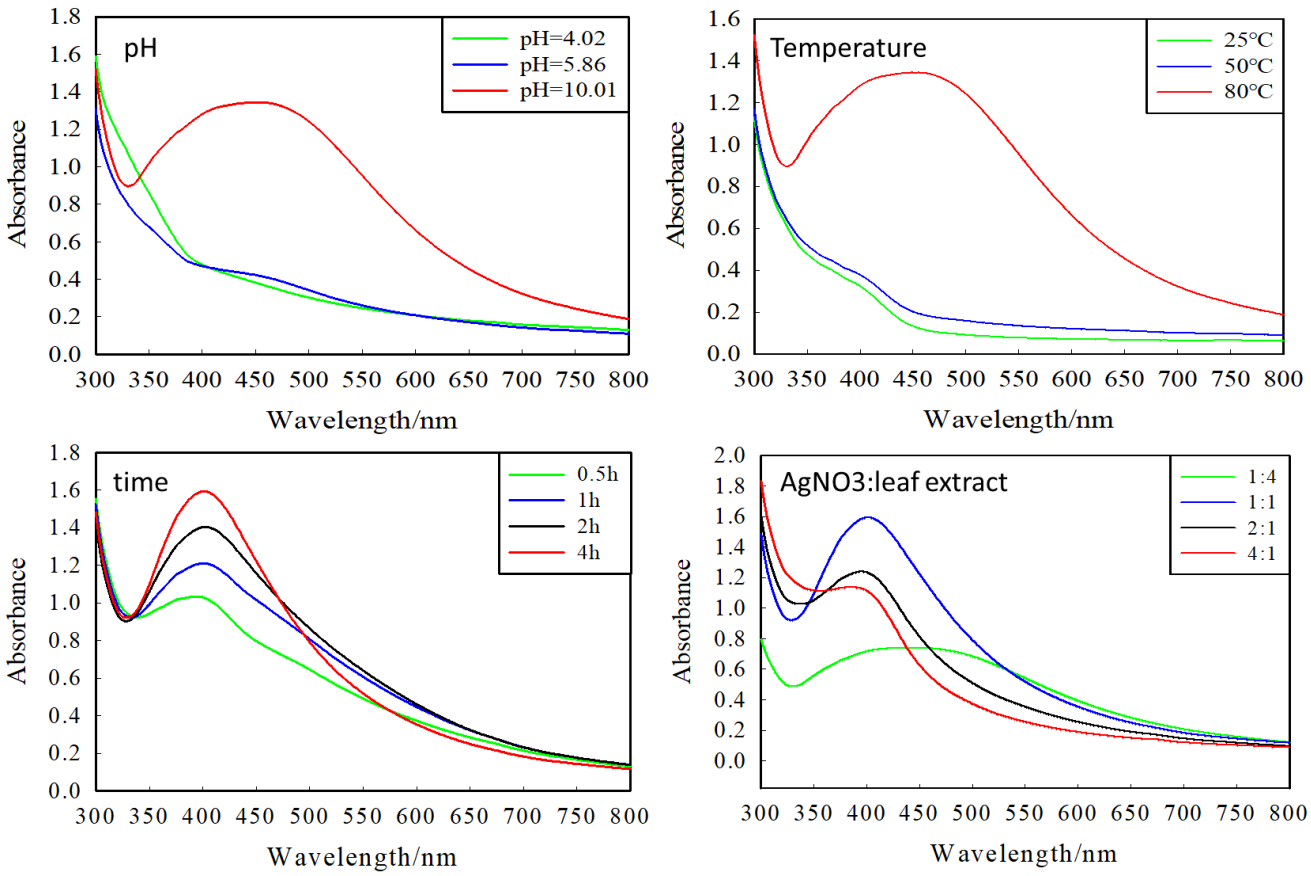

Figure S3. Optimized reaction conditions including pH, temperature, reaction time and the ratio of $AgNO_3$ and leaf extract.

Characterization of Ag Nanoparticles. The newly synthesized NPs were characterized using DLS, TEM, and sp-ICP-MS. The hydrodynamic size and zeta potential of nanoparticles were measured using a Zetasizer Nano ZS (Malvern Instrument, USA). Morphological characteristics were performed using a Transmission Electron Microscope (TEM) (JEM-200CX, JEOL, Japan).

sp-ICP-MS Measurement. An Agilent 7900 ICP-MS (Santa Clara, CA, USA) was used to perform sp-ICP-MS analysis to determine the particle size and concentration of the synthesized AgNPs. Analyses were performed in time resolved analysis (TRA) mode using

an integration time (dwell time) of 100 μs per point with no settling time between measurements. The instrumental settings used for the sp-ICP-MS analysis are summarized in **Table 1**, which were modified based on a previous study.[26] The sp-ICP-MS method setup, data collection, and analysis was conducted via Single Nanoparticle Application Module of the Agilent ICP-MS MassHunter software (Version C.01.04 Build 544.3).

Table 1. The optimized instrumental setting for the AgNPs analysis in sp-ICP-MS

Parameter	Value
RF Power	1550 W
Carrier gas	0.67 L/min
Make-up gas	0 L/min
Spray chamber temperature	2°C
Nebulizer pump	0.1 rps
Sample depth	8.0 mm
Oxide ratio	1 %
Integration time	100 μs
Acquisition time	90 s
Mass monitored	^{107}Ag

An AgNP standard (60 nm, Agilent, USA) was diluted to 100 ng/L Ag (99%) with DI water in metal-free polypropylene tubes, to evaluate the nebulization efficiency, which was used in the data conversion from raw signal to NP size. An Ag ionic standard of 1 μg/L was prepared with 1% HNO_3 and was used to determine the elemental response factor. The samples were diluted with DI water to ensure the AgNPs concentrations were between 50 and 200 ng/L, and a sample inlet flow of 0.346 mL/min was used. Analyte mass fraction was set to 1 while particle density was set to 10.5 g/cm^3. NP sample preparation and dilution were performed on the day of the analysis to avoid sample degradation and minimize transformation of the AgNPs after processing. Before dilution of the samples and

again prior to their analysis, all solutions were placed in an ultrasonic bath for 10 min to ensure that the samples were fully homogenized.

Isothermal titration calorimetry measurement. A TA Instruments Nano Isothermal Titration Calorimeter (nITC) instrument (TA Instruments-Waters LLC, DE, US) was used to measure the heat exchange between Ag^+ and cucumber leaf extracts at 298 K to identify physicochemical interaction as well as determine the thermodynamic data and binding constants.[27]

An Ag^+ solution (1 mM), prepared in degassed DI water (pH 10), was loaded into the 100 μL injection syringe; and a solution of fructose (20 mM) was placed in the 1 mL nITC sample cell (the concentrations of fructose were generally 10-20 times higher than the concentration of Ag^+ to obtain a strong heat exchange signal as well as to ensure reaching interaction equilibrium. The difference in concentrations ratio would not change the output significantly[28].). The rotational speed of the stirrer was 250 min^{-1} to ensure well-mixed. Ag^+ were titrated into the sample cell as a sequence of 20 injections of 4.91 μL aliquots. The equilibrium time between two injections was set at 800 s for the signal to return to the baseline.

Estimated binding parameters were obtained from the nITC data using the NanoAnalyze Data Analysis software (Version 3.60). Data fits were obtained using the independent set of multiple binding sites (MNIS) model[29], for which the analytical solution for the total heat measured, Q (kJ) is determined by the formula:

$$Q = \frac{\left(1+[M]nK_d + K_d[L_T]\right) - \left[\left(1+[M]nK_d + K_d[L_T]\right)^2 - 4[M]nK_d{}^2[L_T]\right]^{1/2}}{\frac{2K_d}{V\Delta H}} \qquad (1)$$

Where V is the volume of the calorimeter cell, ΔH is enthalpy (kJ/mol), and K_d (M^{-1}) is the equilibrium binding constant. Free energy, ΔG (kJ/mol), was determined from the binding constant ($\Delta G = -RT \ln K$, where R is the gas constant and T is the absolute temperature in Kelvin) and entropy, ΔS (kJ/mol), from the second law of thermodynamics ($\Delta G = \Delta H - T\Delta S$). $[L_T]$ is the total ligand concentration and [M] is the macromolecules concentration, n is the molar ratio of interacting species. To consider the j-th injection, the mole ratio can be calculated as:

$$n = \frac{[L_j]}{[M]} \tag{2}$$

with

$$L_j = L_{j-1} + V_j \cdot [L]_m \tag{3}$$

$$M = [M]_m \cdot V \tag{4}$$

where V_j is the volume of each titration, while $[L]_m$ and $[M]_m$ are the molar concentrations of ligand and macromolecules. In the current study, since Ag^+ were titrated into the fructose solution, we considered Ag^+ as a ligand (L), and fructose as macromolecules (M).

Metabolomics to determine molecules responsible for reducing and stabilizing. Metabolites in leaf extracts before and after the reaction were analyzed by GC-MS to determine the metabolites playing key roles in the synthesis of AgNPs.

Sample Preparation. 400 μL extracts were transferred to a 1.5-mL Eppendorf tube, followed by adding 200 μL of chloroform and 20 μL of 2-chloro-l-phenylalanine (0.3 mg/mL) dissolved in methanol as an internal standard. The mixtures were vortexed for 1 min and ultrasonicated for 30 min at ambient temperature. The mixtures were centrifuged

at 12000 rpm for 10 min at 4 °C. An aliquot of the 200 μL supernatant was transferred to a glass sampling vial for vacuum-drying at room temperature. Then 80 μL of 15 mg/mL methoxylamine hydrochloride in pyridine was subsequently added. The resulting mixture was vortexed vigorously for 2 min and incubated at 37 °C for 90 min. Then, 80 μL of N,O-Bis (trimethylsilyl) trifluoroacetamide (BSTFA) (with 1% trimethylchlorosilane) and 20 μL n-hexane were added into the mixture, which was vortexed vigorously for 2 min and then derivatized at 70 °C for 60 min. The samples were placed at room temperature for 30 min before GC-MS analysis.

GC-MS Analysis. The derivatized samples were analyzed in an Agilent 7890B gas chromatography system coupled to an Agilent 5977A mass selective detector (Agilent Technologies Inc., CA, USA). The column was a DB-5MS fused-silica capillary column (30 m × 0.25 mm × 0.25 μm; Agilent Technologies, Santa Clara, CA). Helium (> 99.999%) was used as the carrier gas at a constant flow rate of 1.0 mL/min through the column. The initial oven temperature was 60 °C, ramped to 125 °C at a rate of 8 °C/min, to 210 °C at a rate of 4 °C/min, to 270 °C at a rate of 5 °C/min, to 305 °C at a rate of 10 °C/min, and finally held at 305 °C for 3 min. The injection volume was 1 μL, with the injector temperature at 260 °C and in splitless mode. The temperature of the MS quadrupole and ion source (electron impact) was set to 150 and 230 °C, respectively. The collision energy was 70 eV. Mass data was acquired in a full-scan mode (*m/z* 50-500), and the solvent delay time was set to 5 min. The QCs were injected at regular intervals (every 10 samples) throughout the analytical run to provide a set of data from which repeatability can be assessed. A representative chromatogram (TIC) from GC-MS is shown in **Figure S5**.

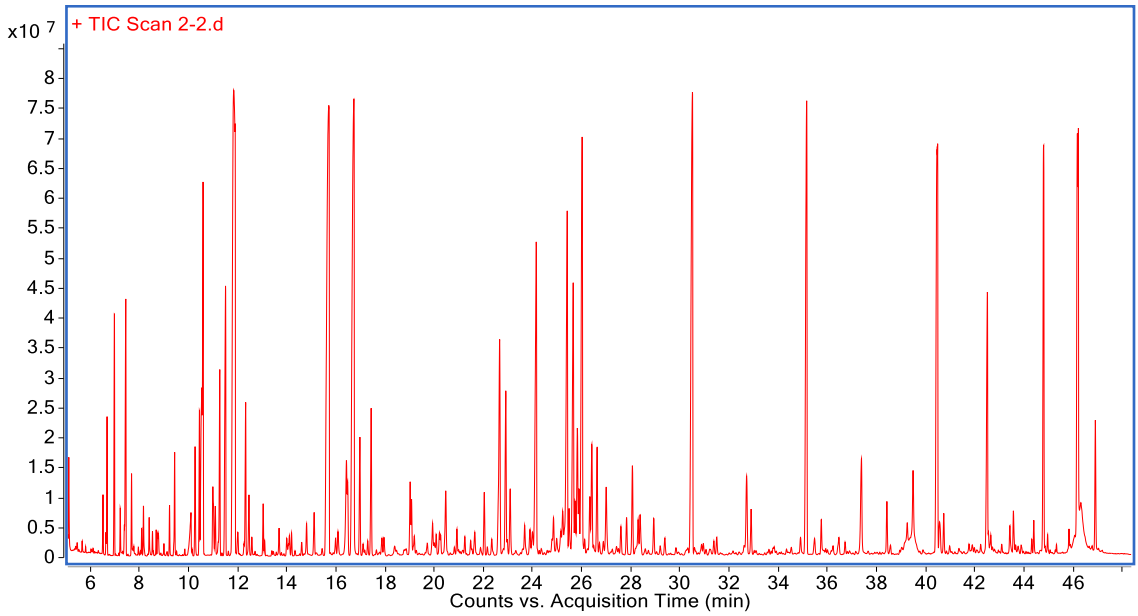

Figure S5. A representative chromatogram (TIC) from GC-MS

Determination of Total Reducing Sugars. Total reducing sugars were determined based on the 3,5-dinitrosalicylic acid (DNS) method.[30] The liquid before and after the reaction was centrifuged at 10000 rpm for 30 min, then 1 mL supernatant was mixed with 2 mL DNS reagent and boiled for 5 min. After cooling the sample down to room temperature, the absorbance was determined at 540 nm with UV-Vis spectrometer (UV-1800, Shimadzu, Japan). The final result was expressed as mg glucose equivalent per mL liquid.

Determination of Total Phenolics. Total phenolics were determined based on the method by Singleton et al..[31] Briefly, 50 μL of the supernatant was mixed with 450 μL of DI water, then 250 μL of 2 M Folin-Ciocalteu reagent and 1.25 mL of 20 g/L Na_2CO_3 were added. The absorbance was measured at 735 nm with UV-Vis spectrometric (UV-1800, Shimadzu, Japan). The final concentration was expressed as μg gallic acid equivalent per mL liquid.

RESULTS AND DISCUSSION

Optimal Conditions for AgNPs Green Synthesis. Preliminary experiments were conducted to optimize synthesis conditions, including pH, reaction time and temperature. Totally 54 trials were completed with various combinations of pH (4.02, 5.86, 10.01), reaction time (0.5, 1, 2, 4h), reaction temperature (25, 50, 80 °C), and $AgNO_3$/leaf extracts ratio (1:4, 1:1, 2:1, 4:1) (**Supporting Information, Figure S1-2**). The approached optimized conditions for AgNP formation: reaction time = 4 h; reaction temperature = 80 °C; pH = 10.01; $AgNO_3$/leaf extracts ratio =1:1 (**Figure S3)**. We found that pH and temperature of the reaction system were the most important factors for the biosynthesis of AgNPs using cucumber leaf extract. Yun et al.[32] hypothesized that a higher pH generates a large number of functional groups, which facilitates a higher number of Ag(I) to bind and subsequently form smaller NPs. Upon mixing of 1.25 mL of 10 mM $AgNO_3$ with 1.25 mL cucumber leaf extracts at 80 °C for 4 h and pH adjusted to 10.0 using 200 µL ammonium hydroxide, the color changed from yellow to yellow-brownish, which indicated the formation of AgNPs (**Figure 1A**). The color change was caused by the surface plasmon resonance (SPR) of AgNPs in the visible region.[33, 34] This plasmon resonance is an intrinsic property of AgNPs and arises from the coupling between the electron cloud on the surface of AgNPs with the incident electromagnetic radiation. Therefore, the color change is a clear indicator of AgNP formation. The formation of AgNPs in reaction solution was further confirmed by UV-Visible spectroscopy. A single sharp intense peak at 414 nm (**Figure 1 A**) was observed, suggesting the existence of AgNPs, since the characteristic peak of AgNPs is between 380 to 420 nm depending on the size of the AgNPs.[35, 36]

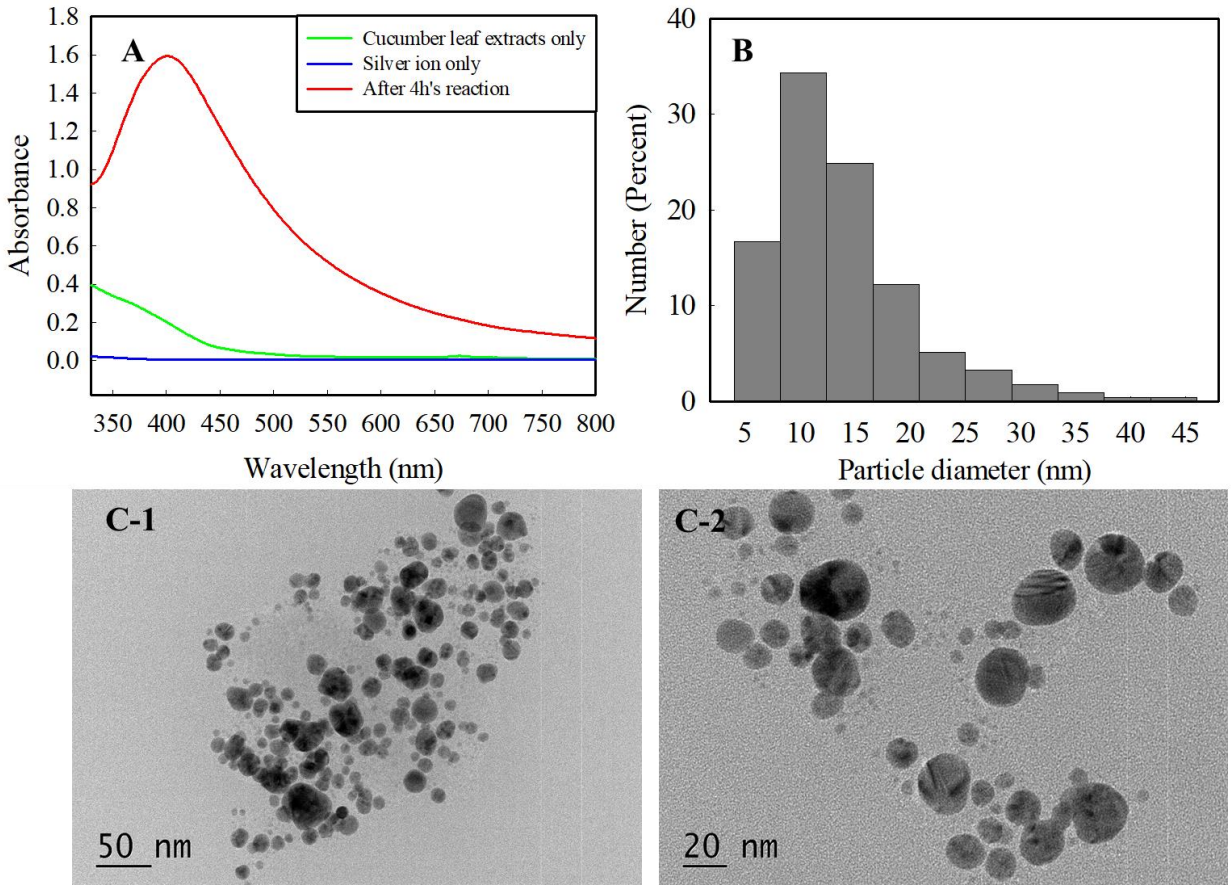

Figure 1. (**A**) UV-vis spectrum of AgNPs synthesized by reduction of aqueous Ag ion solution with the cucumber leaf extract (pH 10, reaction temperature 80 °C, reaction time 4h, $AgNO_3$:leaf extract=1:1). (**B**) TEM size distribution of AgNPs. **(C)** Representative TEM images of the AgNPs prepared using cucumber leaf extracts with a scale bar of (C-1) 1 μm (20,000 × magnification); and(C-2) 100 nm (37,000 × magnification).

AgNPs Characterization. The particle size distribution of the synthesized AgNPs in suspension was determined by TEM and DLS. A typical TEM image reveals that the particles were roughly spherical in shape with a size range between 5 ~ 25 nm (average size 13.7 nm) (**Figure 1 B and C)**. The average hydrodynamic diameter of the AgNPs in

DI water is 75.7±2.8 nm, with a zeta potential of -19.82±0.11 mV. To investigate the stability of AgNPs, hydrodynamic size and zeta potential were monitored in 0, 7, 14 and 36 days. Results showed that the hydrodynamic size of AgNPs was stable within 36 days, indicating high stability of the synthesized NPs (**Figure S4**).

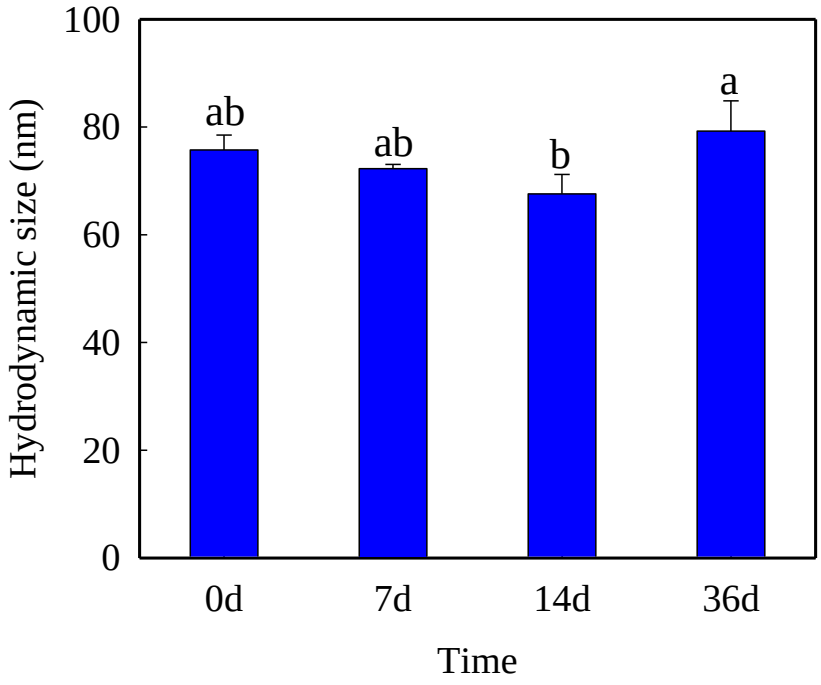

Figure S4. Stability (hydrodynamic size changes) of the obtained AgNP. The hydrodynamic size of AgNP was determined at day 0, 7, 14 and 36. AgNPs was fabricated by adding 1.25 mL $AgNO_3$ NPs to 1.25 mL cucumber leaf extracts at pH 10, react for 4 h at 80 °C.

Transformation process from Ag ion to AgNPs. sp-ICP-MS was employed to obtain more detailed information regarding the particle number, mass concentration, particle size, and elemental composition of the synthesized AgNPs, which was conducted in a time-dependent setup (**Figure 2**) to investigate the nucleation and crystal growth. After heating

at 80 °C with cucumber leaf extracts for 30 min, AgNPs with a most frequent size of 40.67±1.15 nm were detected (**Table 2**), indicating fast nucleation of AgNPs. Noticeably, there was a small portion of AgNPs with size larger than 100 nm as shown in the blue bar in **Figure 2A**. With increasing reaction time, the size of the AgNPs continued to increase; the largest mean size (76.42±1.33 nm) was achieved after 4 h reaction (**Table 2**). However, even after 4 h reaction, the most frequent size was determined to almost unchanged (42.00±2.00 nm) compared to that (40.67±1.15 nm) at 30 min reaction time. It suggested that most of the newly synthesized AgNPs show a relatively narrow size distribution, which would not be affected by the reaction time. The mean size of AgNPs increased from 58.06±0.29 nm to 76.42±1.33 nm as the reaction proceeded (**Figure 2**), which was consistent with the DLS measurements. As reaction time been extended, the portion of larger size (>100 nm) AgNPs significantly increased, shown as the blue bars in **Figure 2**, which indicated a time-depend AgNPs crystal growth. The concentration of synthesized AgNPs increased from 51.76 to 219.32 mg/L, meanwhile, the concentration of Ag ions decreased from 215.80 to 46.33 mg/L at the end of the 4 h reaction time (**Figure 3**), which suggested that Ag^{+} ions were sequentially transformed to AgNPs during the green synthesis process. This demonstrates that the current green synthesis is a rapid (>0.5-4 h) and efficient way to prepare AgNPs with the yield rate of 49.19±0.66%.

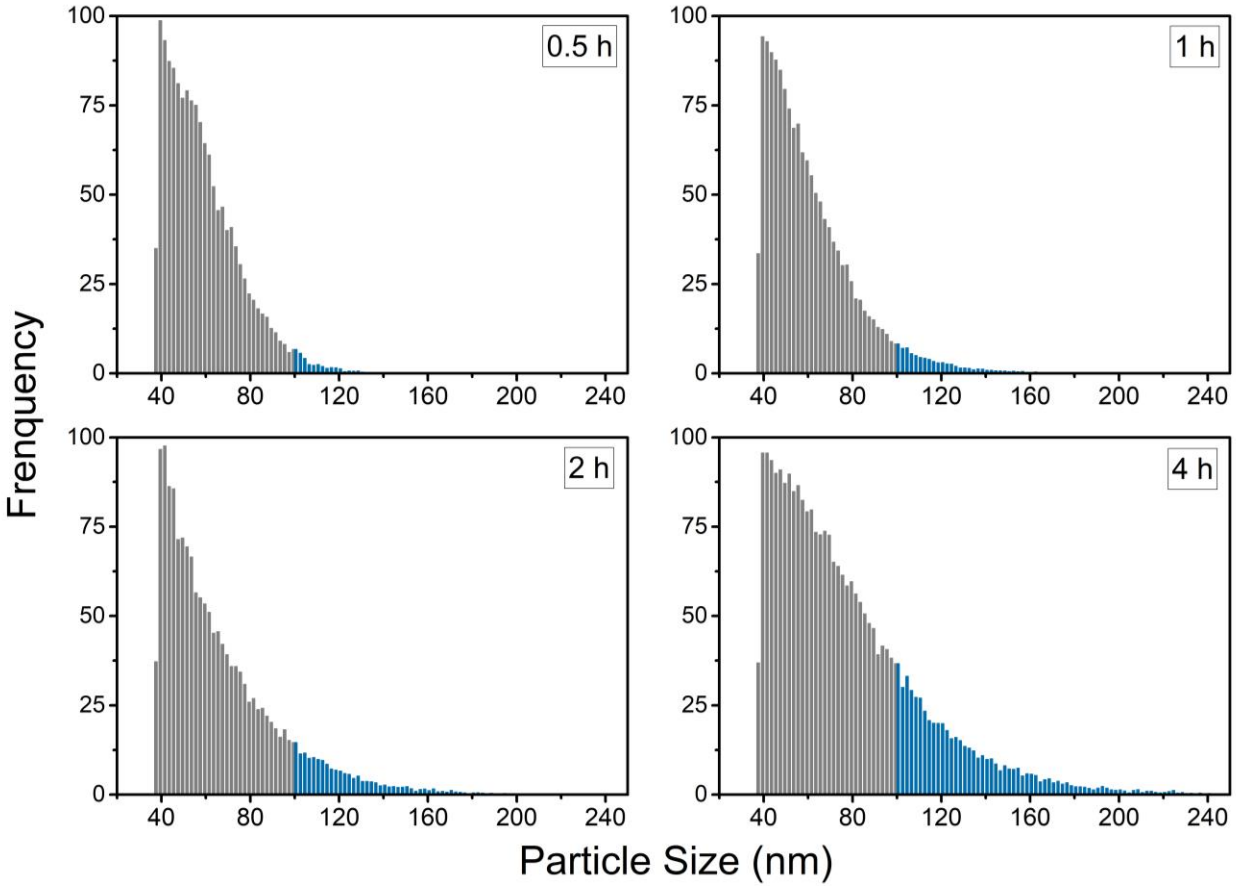

Figure 2. Size distribution measured via sp-ICP-MS of AgNPs synthesized by cucumber leaf extract at 80 °C after (A) 30 min; (B) 1 h; (C) 2 h and (D) 4 h. The blue bars represent the frequency of AgNPs with a size larger than 100 nm.

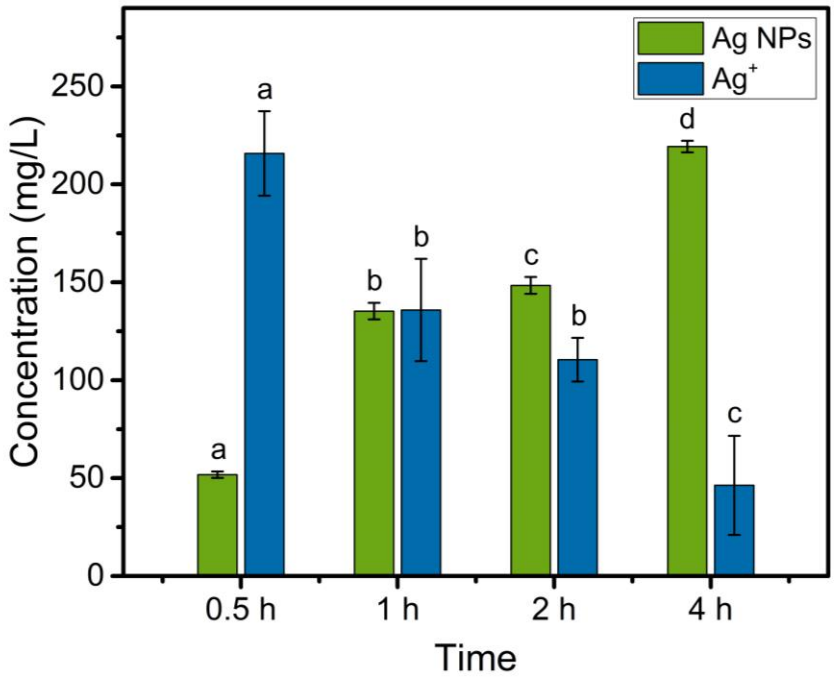

Figure 3. AgNP and Ag ions concentration measured via sp-ICP-MS at different synthesis time (30 min, 1 h, 2 h and 4 h). The AgNPs were synthesized by adding 1.25 mL of leaf extract to 1.25 mL of $AgNO_3$ and heated at 80 °C and pH 10. Data are the mean of three replicates, and error bars represent ± standard error. Different letters stand for statistical differences at $p \leq 0.05$ (Tukey's HSD multiple comparisons at $p \leq 0.05$).

Table 2. Median, mean, and most frequent size of AgNPs synthesized with cucumber leaf extract at different reaction time, as measured by sp-ICP-MS. (The values of average and standard deviation were calculated from triplicate measurements)

Reaction time	Median size (nm)		Mean size (nm)		Most Frequent size (nm)	
(h)	Avg.	Std.	Avg.	Std.	Avg.	Std.
0.5	54.63	0.20	58.06	0.29	40.67	1.15
1	55.32	0.42	60.31	0.49	40.67	1.15
2	58.10	0.18	65.45	0.26	41.33	1.15
4	68.52	1.26	76.42	1.33	42.00	2.00

Metabolites Responsible for Ag Nanoparticle Formation. Cucumber plants contain various metabolites including sugars, amino acids, phenolics, fatty acids, and other secondary metabolites. A variety of metabolites have the ability to reduce the Ag^+ to Ag(0), such as sugars, ascorbic acid, and phenolics. **Table 3** presents the relative concentration of metabolites before and after the reaction, from the GC-MS based metabolomics. We considered that metabolites with a concentration decrease higher than 1.2 folds were responsible for the reactions, and can either act as reducing or stabilizing agents. There were in total 40 compounds which relative concentrations were significantly (p<0.05) decreased (**Table 3**). Most of the significantly changed metabolites were sugar and organic acid, indicating sugar and organic acid played important role in reducing Ag ions to AgNP.

Table 3. Relative abundance of metabolites before and after reaction during formation of AgNPs. (The relative abundance values were reported as the "average ± standard deviation" of three replicates.)

Metabolites	Classification	Relative Abundance		Fold
		Before	After	
2-Amino-2-Norbornanecarboxylic Acid	Organic acid	1.47±0.01	0.00±0.00	
Cellobiose	Sugar	4.94±0.52	0.00±0.00	
Biuret		2±0.02	0.06±0.09	31.5
D-Glucoheptose	Sugar	6.85±0.54	0.72±0.04	9.6
Pyruvic Acid	Organic acid	49.22±2.33	6.63±2.07	7.4
Alpha-Ketoglutaric Acid	Organic acid	4.66±0.66	0.81±0.26	5.8
2-Amino-2-Methylpropane-1,3-Diol		7.35±0.04	1.56±0.39	4.7
Glucoheptonic Acid	Organic acid	205.29±13.7	77.19±20.28	2.7
N-Acetyl-L-Glutamic Acid	Organic acid	35.92±3.94	15.7±2.15	2.3
5-Aminoimidazole-4-Carboxamide		0.96±0.03	0.42±0.01	2.3
1-Methylhydantoin		71.86±2.69	33.39±2.39	2.2
Cumic Acid	Organic acid	3.48±0.07	1.67±0.03	2.1
L-Allothreonine		36.99±0.2	18.44±6.49	2.01
N-Acetyl-5-Hydroxytryptamine		2.14±0.08	1.06±0.04	2.0
Melibiose	Sugar	9.9±0.44	5.27±0.65	1.9
2-Deoxy-D-Glucose	Sugar	7.18±0.45	3.85±0.58	1.9
Hesperitin		0.11±0.02	0.06±0.01	1.88
Tagatose	Sugar	203.88±8.39	111.95±15.98	1.8
Dibenzofuran		13.63±0.94	7.83±0.34	1.7
Farnesol	Alcohol	0.28±0.01	0.17±0.00	1.7
Benzoylformic Acid	Organic acid	0.38±0.01	0.23±0.04	1.6
Squalene	Alkene	0.37±0.01	0.23±0.01	1.6
Methyl Octanoate	Ester	4.37±0.12	2.71±0.03	1.6
Indole-3-Acetamide		0.77±0.09	0.49±0.03	1.6
Alpha-Ketoisocaproic Acid	Organic acid	4.46±0.25	2.82±0.28	1.6
N,N-Dimethylarginine		5.65±0.33	3.58±0.36	1.6
P-Benzoquinone		25.69±0.85	16.34±0.51	1.6
Fructose	Sugar	291.27±12.51	186.66±27.54	1.6
2-Keto-Isovaleric Acid	Organic acid	1.68±0.07	1.08±0.16	1.6
Stearic Acid	Fatty acid	0.85±0.14	0.57±0.05	1.51
Nicotinoylglycine		1.81±0.07	1.17±0.03	1.5
4-Hydroxymethyl-3-Methoxyphenoxyacetic Acid	Organic acid	0.52±0.01	0.34±0.03	1.5
2-Aminoethanethiol		26.57±0.54	17.83±0.57	1.5
Palmitic Acid	Fatty acid	1.11±0.14	0.77±0.02	1.44
N-Alpha-Acetyl-L-Ornithine	Organic acid	17.97±1.22	12.66±0.94	1.4
Pelargonic Acid	Organic acid	0.27±0.01	0.19±0.01	1.4
Aminomalonic Acid	Organic acid	0.30±0.00	0.23±0.01	1.4
Ribose	Sugar	35.58±1.17	26.33±2.83	1.4
3-Methylamino-1,2-Propanediol	Alcohol	2.22±0.07	1.68±0.15	1.3
3,6-Anhydro-D-Galactose	Sugar	24.64±0.22	20.07±0.50	1.2

Sugars and sugar alcohols. It is interesting to note that a number of sugar and sugar derivatives, such as cellobiose, d-glucoheptose, ribulose-5-phosphate, melibiose, 2-deoxy-D-glucose, tagatose, fructose, ribose, 3,6-anhydro-D-galactose (**Figure 4**) were significantly (p<0.05) decreased after the reaction. Those sugar and sugar derivatives were possibly involved in the formation of AgNPs and likely function as a reducing agent. Shankar et al. hypothesized that reducing sugars in Neem leaf extract could be responsible for the reduction of metal ions to the corresponding metal NPs.[37] However, this hypothesis was not proven valid for Neem leaf extract. Not surprisingly, non-reducing sugar like sucrose, were unchanged in the cucumber leaf extracts after the reaction. In addition, sugar alcohols like mannitol, threitol and galactinol (**Table S1**) were unchanged, indicating they did not participate in the reaction. We further analyzed total reducing sugar before and after reaction with cucumber leaf extract. We hypothesized that total reducing sugars should decrease during the formation of AgNPs. Surprisingly, total reducing sugars content increased by 227% after the reaction, which could be due to that polysaccharides were degraded into reducing single sugars, thus maintaining a high level of total reducing sugars.

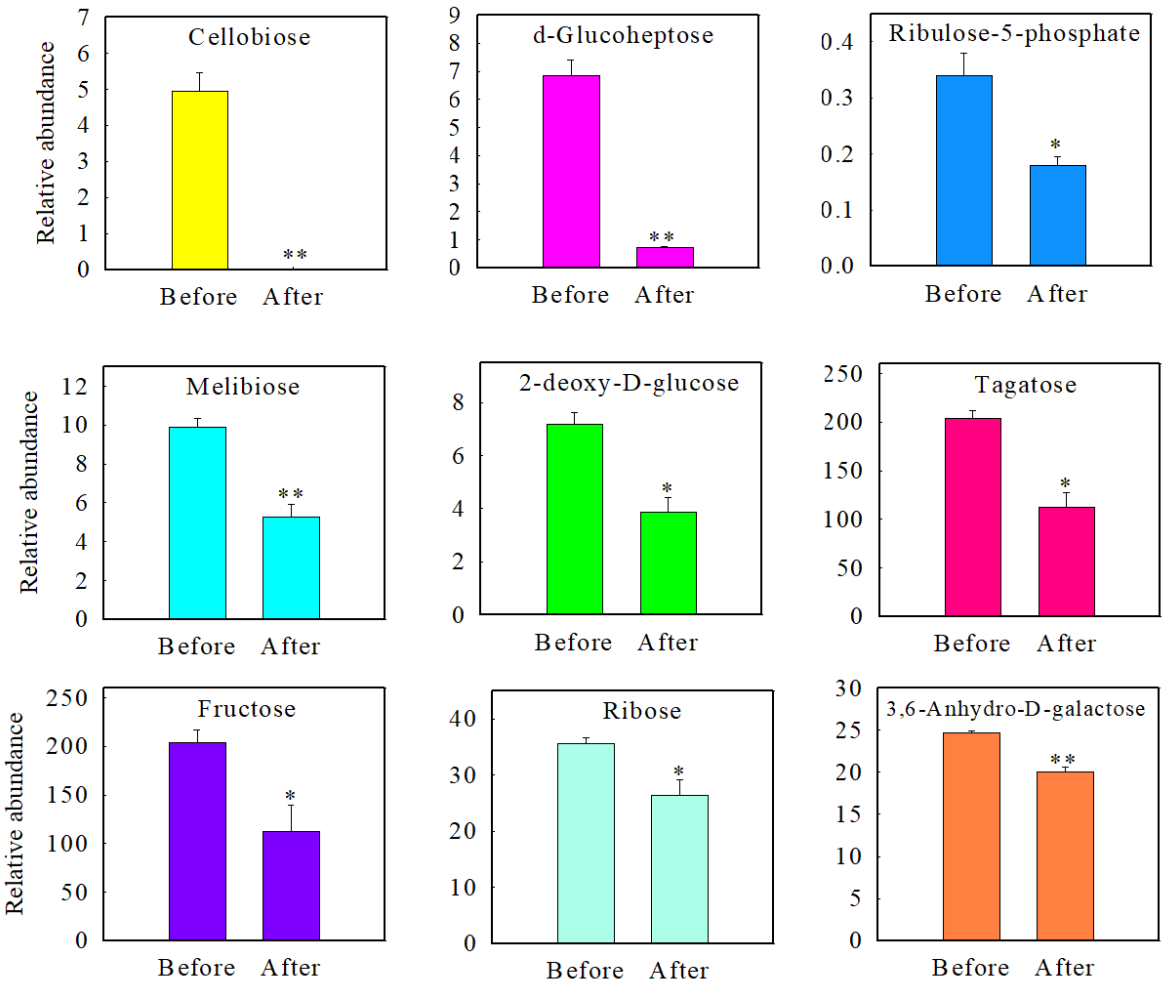

Figure 4. The relative abundance of significantly changed sugars determined by GC-MS in solution before and after the reaction. The AgNPs were synthesized by adding 1.25 mL of leaf extract to 1.25 mL of $AgNO_3$ and heated at 80 °C and pH 10.

Table S1. Relative abundance of metabolites before and after reaction during formation of AgNPs. (The relative abundance values were reported as the "average ± standard deviation" of three replicates.)

Metabolites	Classification	Relative Abundance		Fold
		Before	After	
Alanine	Amino acid	7.89±0.49	7.21±0.03	1.1
Beta-Mannosylglycerate	Ester	485.13±25.25	444.95±38.14	1.1
N-Acetylisatin	Amino acid	0.96±0.05	0.88±0.15	1.1
N-Methyl-L-Glutamic Acid		13.02±0.28	12±1	1.1
Ethanolamine		253.05±10.65	234.51±9.32	1.1
Fucose	Sugar	24.85±0.79	23.2±1.95	1.1
D-Arabitol	Sugar alcohol	10.23±0.01	9.66±0.24	1.1
Aminooxyacetic Acid	Organic acid	2.96±0.05	2.81±0.07	1.1
Sorbitol	Sugar alcohol	5.15±0.01	4.89±0.12	1.1
Valine	Amino acid	189.21±1.34	180.72±3.28	1.0
D-Talose	Sugar	127.73±5.17	122.64±18.29	1.0
Galactinol		266.67±8.32	259.61±0.01	1.0
Glycine	Amino acid	305.63±1.75	299.35±0.65	1.0
Glucosaminic Acid	Organic acid	2.39±0.04	2.35±0.05	1.0
Glycerol	Alcohol	264.3±1.2	262.4±2.88	1.0
Norvaline	Amino acid	0.39±0.05	0.39±0.01	1.0
3-Hydroxypyridine		1.68±0.18	1.67±0.01	1.0
Diglycerol	Alcohol	5.37±0.05	5.35±0.15	1.0
1,5-Anhydroglucitol	Sugar alcohol	0.24±0.02	0.24±0.01	1.0
22-Ketocholesterol		1.76±0.41	1.76±0.04	1.0
O-Succinylhomoserine		0.23±0	0.23±0	1.0
2-Furoic Acid	Organic acid	1.84±0.24	1.84±0.08	1.0
Gluconic Lactone	Ester	7.45±0.15	7.65±0.01	1.0
Citramalic Acid	Organic acid	26.36±0.13	27.23±0.58	1.0
Ribonic Acid, Gamma-Lactone		0.74±0.02	0.78±0.02	1.0
Mannitol	Sugar alcohol	11.34±0	11.88±0.39	1.0
Tyrosine	Amino acid	32.89±0.09	34.58±1.9	1.0
Citric Acid	Organic acid	401.56±12.5	423.38±2.28	0.9
D-Erythro-Sphingosine		15.61±0.45	16.65±0.25	0.9
Nicotinic Acid	Organic acid	15.49±2.03	16.56±0.07	0.9
3-Hydroxybutyric Acid	Organic acid	0.17±0.01	0.18±0.01	0.9
2-Methylglutaric Acid	Organic acid	0.96±0.02	1.05±0	0.9
Leucrose	Sugar	0.16±0.01	0.17±0.01	0.9
O-Acetylserine		4.15±0.18	4.56±0.23	0.9

To further investigate the role of the sugars as the reducing agent in AgNPs green synthesis process, ITC was applied to identify and detect the physicochemical interactions between cucumber leaf extracts and Ag^+. Base on the metabolomics screening results and our hypotheses, we chose fructose as a case study to discuss the sugars were acting as reducing agents from the thermodynamic perspective.[27] The heat exchange as a function of time as Ag^+ was titrated into the fructose solution was shown in the real-time thermogram (**Figure 5 A**). Each injection of Ag^+ results in heat change due to the binding between Ag^+ and fructose within the sample cell, causing a change in the heat flow, shown as peaks in the thermogram (**Figure 5 A**). The interaction between Ag^+ and fructose was exothermic, and the peak amplitudes and area gradually decreased as more Ag^+ was added since the number of available binding sites decreased. Eventually, only a low heat exchange was observed for the last several injections corresponding to dilution, once binding sites were saturated.

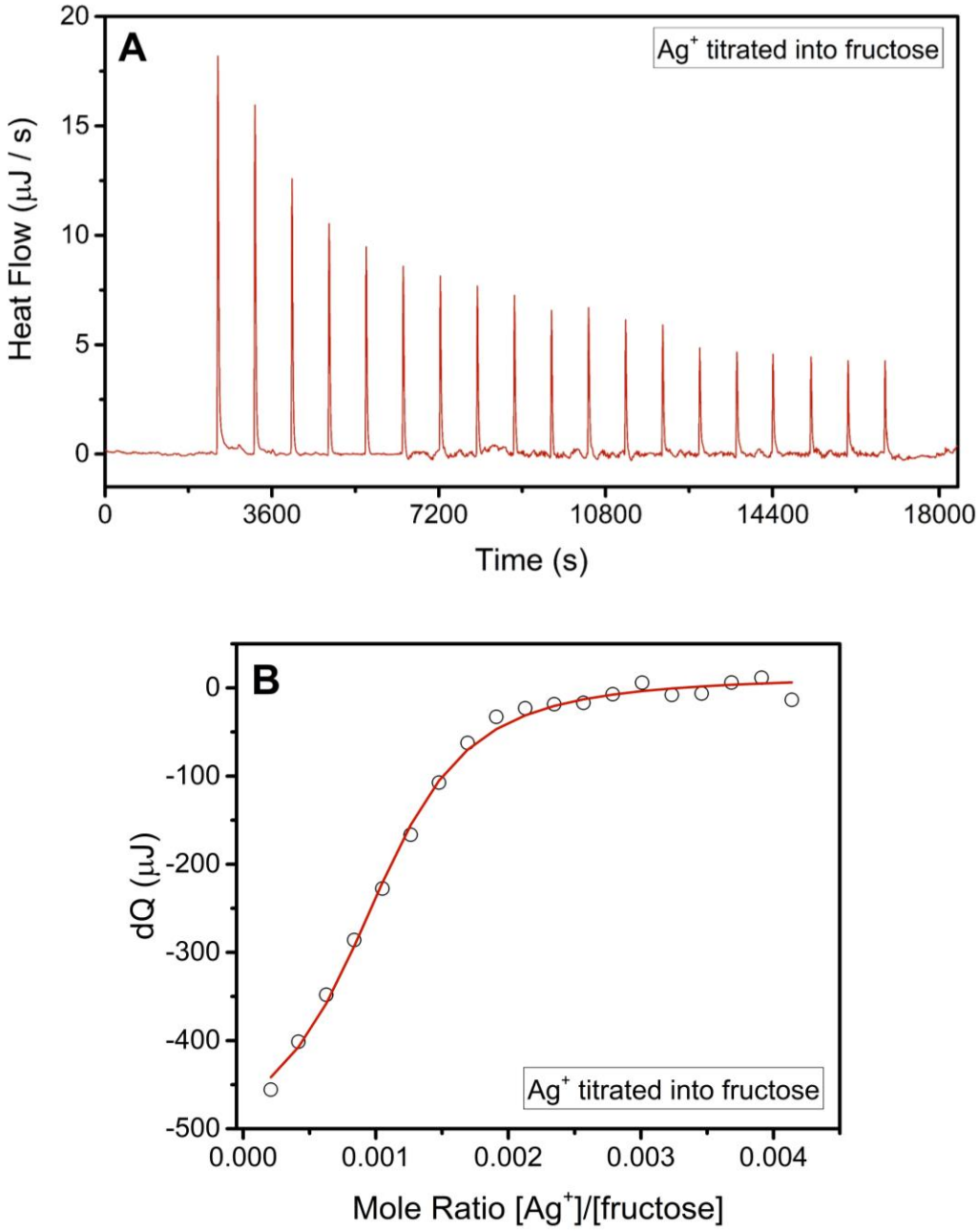

Figure 5. (A) Thermograms for Ag^+ titration into fructose solutions at 298 K. Heat flow reflects the differential signal, with positive peaks indicating an exothermic process; (B) Integrated heat data as a function of mole ratio of Ag^+ to fructose, fitted with MNIS model. Symbols represent experimental data, and red lines represent model prediction.

The energy exchange as a function of the ratio between Ag^+ and fructose was presented in **Figure 5 B**. The independent set of multiple binding sites (MNIS) model (eq 1)[29] was applied to process the data, and the fitted and calculated thermodynamic parameters suggested that the interaction between Ag^+ and fructose were thermodynamically identical. It's energetically favored spontaneous processes with $\Delta G = -30.45$ kJ/mol, and the interactions were enthalpically driven with negative ΔH value (-109.8 kJ/mol). The stoichiometric values (n=0.001) was much smaller than unity the stoichiometric values are much smaller than unity, indicating that due to the relatively low reducing power, more fructose molecular were involved in the reduction process.

Thus, the ITC results demonstrate the important role of the sugars from cucumber leaf extracts in the AgNPs green synthesis process.

Phenolics. Phenolic compounds possess hydroxyl and carboxyl groups, and may inactivate metal ions by chelating and additionally suppressing the superoxide-driven Fenton reaction, which is believed to be the most important source of reactive oxygen species (ROS). Therefore, plants with high content of phenolic compounds (e.g. Pinus species) are some of the best candidates for nanoparticle synthesis.[3] It has been reported that polyphenols can be adsorbed on the surface of metallic nanoparticles through the interaction with their carbonyl groups.[14] The mechanism of converting ketone groups to carboxylic acid in flavonoids was proposed to play an important role during the conversion of Ag^+ to Ag. Unexpectedly, all of the detected phenolic compounds, including 1,2,4-benzenetriol, caffeic acid, ferulic acid, hydrocinnamic acid, were unchanged during the reaction (**Table S1**), which indicated that these compounds did not participate in the

reaction. We further determined total phenolics in the system before and after the reaction, and we found no changes in total phenolics content. This further confirmed that phenolic compounds did not play a role in the process of reducing Ag ions to AgNPs.

Amino acids. The levels of most amino acids, including alanine, asparagine, lysine, valine, isoleucine, proline, serine, threonine, beta-alanine, tyrosine, tryptophan, were unchanged after reaction in this study (**Table S1**). This indicates that amino acids did not play important role in the reduction of Ag ion to AgNPs. Gruen[38] reported that arginine, cysteine, lysine and methionine, out of twenty amino acids, were able to interact with Ag^+.

Organic acids. Pyruvic acid, generated from the redox reactions in the glycolytic pathway, was decreased 7-fold after reaction (**Table 3**), indicating it participated in the synthesis, possibly acting as a reducing agent[14]. In addition to pyruvic acid, 2-Amino-2-norbornanecarboxylic acid, alpha-ketoglutaric acid, glucoheptonic acid, N-Acetyl-L-glutamic acid, cumic acid decreased approximately 2- and 6- fold, respectively, which indicates these two carbohydrate acids likely participated in the formation of AgNPs.

Citric acid and oxalic acid have been hypothesized to be involved in the reduction of Ag^+ to AgNPs.[39, 40] Prathna et al.[40] predicted that citric acid could act as both the principal reducing agent and stabilizing agent during AgNP synthesis. In our study, neither oxalic nor citric acid changed their concentration, indicating they were not involved in the reduction and that citric acid or citrate would not be the principal stabilizing agent in a more complex mixture of organic compounds such as cucumber leaf extract (**Table 3**).

Fatty acid. Interestingly, two saturated fatty acids stearic acid and palmitic acid exhibited concentration decreases approximately 1.5-fold after reaction (**Table 3**). Since it

is unlikely that these fatty acids would have the capacity to reduce Ag^+ to Ag, we hypothesize that they act as capping agents on the surface of AgNPs. A previous study indicated that fatty acids can act as stabilizing agents in the synthesis of silver nanoparticles.[41-43] Nagasawa et al., showed that coating silver nanoparticles with fatty acids (myristic, stearic and oleic acid) stabilized the nanoparticles, preventing their aggregation.[41]

In summary, through GC-MS based metabolomics a number of metabolites were found to be responsible for reducing of Ag ion to AgNPs. But it has to be noted that higher molecular weight compounds such as proteins may also play an important role in forming AgNPs. Previous studies reported that proteins can bind to Au nanoparticles through their free amine groups or carboxylate ions.[14] Bali et al. proposed that protein not only act as reducing agent, but also can act as stabilizing agents.[44] The role of the protein, even polysaccharide may act as reducing agent in nanoparticles biosynthesis, which need to be explored in future study.

CONCLUSION

A simple one-pot green synthesis method using the cucumber leaf extract to prepare AgNPs was developed. The formation kinetics of AgNPs was investigated via sp-ICP-MS, suggesting a fast generation process (less than 30 min). The synthesized AgNPs were stable, and no agglomerations were found in the 36-day period. GC-MS based metabolomics screened out the responsible metabolites in the green synthesis process. Specific reducing sugars (e.g., cellobiose, fructose, ribose and et. Al) and some organic

acids were were remarkably decreased during the green synthesis process, indicating the consumption of metabolites in the AgNPs formation. The metabolomics results provided very valuable information with regards to the metabolites responsible for reducing Ag^+ and stabilizing the AgNPs. This is the first report that determines the key metabolites in a green synthesis method for AgNPs. The significant role of sugar in the biosynthesis of AgNPs were further thermodynamically identical via ITC measurement. A thorough understanding of the underlying mechanisms involved in the synthesis process will enable this approach to be economically competitive with conventional methods.

Supporting Information

Table S1 presents a relative abundance of metabolites before and after reaction during formation of AgNPs; Table S2 and S3 presents the process of optimization of reaction conditions, including pH, reaction temperature, reaction time and the ratio of $AgNO_3$ and leaf extracts. Figure S1-3 shows trials to optimize the reaction condition; Figure S4 shows the stability of the synthesized AgNPs; Figure S5 is a representative chromatogram (TIC) from GC-MS.

Conflicts of interest

There are no conflicts of interest to declare.

Acknowledgements

This work was supported by the National Key Research and Development Program of China under 2016YFD0800207. We also acknowledge the National Natural Science Foundation of China under 21876081. Any opinions, finding, and conclusions or recommendations expressed in this material are those of authors and do not necessarily reflect the views of National Science Foundation of China. Arturo Keller thanks Agilent Technologies for the Agilent Thought Leadership award, which partially supported this work. Part of this work was supported by the National Science Foundation (NSF) and the U.S. Environmental Protection Agency (EPA) under NSF-EF0830117. The MRL Central Facilities supported by the MRSEC Program of the National Science Foundation under awards NO. DMR 1121053; a member of the NSF-funded Materials Research Facilities Network (www.mrfn.org). We thank the MRL Central Facilities for the use of their ITC

REFERENCES

1. P. P. Gan and S. F. Y. Li, *Reviews in Environmental Science and Bio/Technology*, 2012, **11**, 169-206.
2. J. R. Peralta-Videa, Y. Huang, J. G. Parsons, L. Zhao, L. Lopez-Moreno, J. A. Hernandez-Viezcas and J. L. Gardea-Torresdey, *Nanotechnology for Environmental Engineering*, 2016, **1**, 1-29.
3. S. Iravani, *Green Chem*, 2011, **13**.
4. J. R. Peralta-Videa, Y. Huang, J. G. Parsons, L. Zhao, L. Lopez-Moreno, J. A. Hernandez-Viezcas and J. L. Gardea-Torresdey, *Nanotechnology for Environmental Engineering*, 2016, **1**, 4.
5. S. Iravani, *Green Chemistry*, 2011, **13**, 2638-2650.
6. S. S. Momeni, M. Nasrollahzadeh and A. Rustaiyan, *Journal of Colloid and Interface Science*, 2017, **499**, 93-101.
7. M. Maham, M. Nasrollahzadeh, S. M. Sajadi and M. Nekoei, *Journal of Colloid and Interface Science*, 2017, **497**, 33-42.
8. S. Ahmed, Annu, S. Ikram and S. Yudha S, *Journal of Photochemistry and Photobiology B: Biology*, 2016, **161**, 141-153.

9. Annu, A. Ali and S. Ahmed, in *Handbook of Ecomaterials*, eds. L. M. T. Martínez, O. V. Kharissova and B. I. Kharisov, Springer International Publishing, Cham, 2018, pp. 1-45.
10. S. Ahmed, Annu, I. Zafeer and S. Ikram, *Journal of Bionanoscience*, 2016, **10**, 47-53.
11. Annu, S. Ahmed, G. Kaur, P. Sharma, S. Singh and S. Ikram, *Toxicology Research*, 2018, **7**, 923-930.
12. Annu, S. Ahmed, G. Kaur, P. Sharma, S. Singh and S. Ikram, *Journal of Applied Biomedicine*, 2018, **16**, 221-231.
13. M. S. Akhtar, J. Panwar and Y.-S. Yun, *ACS Sustainable Chemistry & Engineering*, 2013, **1**, 591-602.
14. P. P. Gan and S. F. Y. Li, *Rev Environ Sci Biotechnol*, 2012, **11**.
15. R. Mohammadinejad, S. Karimi, S. Iravani and R. S. Varma, *Green Chemistry*, 2016, **18**, 20-52.
16. D. Hebbalalu, J. Lalley, M. N. Nadagouda and R. S. Varma, *ACS Sustainable Chemistry & Engineering*, 2013, **1**, 703-712.
17. R. G. Haverkamp and A. T. Marshall, *Journal of Nanoparticle Research*, 2009, **11**, 1453-1463.
18. L. Marchiol, A. Mattiello, F. Pošćić, C. Giordano and R. Musetti, *Nanoscale Research Letters*, 2014, **9**, 101.
19. G. A. Kahrilas, L. M. Wally, S. J. Fredrick, M. Hiskey, A. L. Prieto and J. E. Owens, *ACS Sustainable Chemistry & Engineering*, 2014, **2**, 367-376.
20. N. A. Begum, S. Mondal, S. Basu, R. A Laskar and D. Mandal, *Biogenic synthesis of Au and Ag nanoparticles using Aqueous solutions of Black Tea leaf extracts*2009.
21. L. Zhao, Y. Huang, J. Hu, H. Zhou, A. S. Adeleye and A. A. Keller, *Environmental Science & Technology*, 2016, **50**, 2000-2010.
22. L. Zhao, Y. Huang, H. Zhou, A. S. Adeleye, H. Wang, C. Ortiz, S. Mazer and A. A. Keller, *Environ. Sci.: Nano*, 2016, **3**, 1114-1123.
23. Y. Huang and A. A. Keller, *Environ. Sci.: Nano*, 2016, **3**, 1206-1214.
24. L. Zhao, Y. Huang and A. A. Keller, *Journal of Agricultural and Food Chemistry*, 2018, **66**, 6628-6636.
25. L. Zhao, Y. Huang and A. A. Keller, *Journal of Agricultural and Food Chemistry*, 2017.
26. A. A. Keller, Y. Huang and J. Nelson, *Journal of Nanoparticle Research*, 2018, **20**, 101.
27. Y. Huang, L. Zhao and A. A. Keller, *Environ. Sci. Technol.*, 2017, **51**, 9774-9783.
28. W. B. Turnbull and A. H. Daranas, *J. Am. Chem. Soc.*, 2003, **125**, 14859-14866.
29. E. Freire, O. L. Mayorga and M. Straume, *Anal. Chem.*, 1990, **62**, 950A-959A.
30. M. Ma, P. Wang, R. Yang and Z. Gu, *Food chemistry*, 2018, **250**, 259-267.
31. V. L. Singleton and J. A. Rossi, *American Journal of Enology and Viticulture*, 1965, **16**, 144-158.
32. M. Sathishkumar, K. Sneha, S. W. Won, C. W. Cho, S. Kim and Y. S. Yun, *Colloids and Surfaces B: Biointerfaces*, 2009, **73**, 332-338.

33. E. C. Njagi, H. Huang, L. Stafford, H. Genuino, H. M. Galindo, J. B. Collins, G. E. Hoag and S. L. Suib, *Langmuir*, 2011, **27**, 264-271.
34. J. Xie, J. Y. Lee, D. I. C. Wang and Y. P. Ting, *ACS Nano*, 2007, **1**, 429-439.
35. N. Aihara, K. Torigoe and K. Esumi, *Langmuir*, 1998, **14**, 4945-4949.
36. S. Alipilakkotte and L. Sreejith, *Materials Letters*, 2018, **217**, 33-38.
37. S. S. Shankar, A. Rai, A. Ahmad and M. Sastry, *Journal of Colloid and Interface Science*, 2004, **275**, 496-502.
38. L. Clem Gruen, *Biochimica et Biophysica Acta (BBA) - Protein Structure*, 1975, **386**, 270-274.
39. A. D. Dwivedi and K. Gopal, *Colloids and Surfaces A: Physicochemical and Engineering Aspects*, 2010, **369**, 27-33.
40. T. C. Prathna, N. Chandrasekaran, A. M. Raichur and A. Mukherjee, *Colloids and Surfaces B: Biointerfaces*, 2011, **82**, 152-159.
41. H. Nagasawa, M. Maruyama, T. Komatsu, S. Isoda and T. Kobayashi, *physica status solidi (a)*, 2002, **191**, 67-76.
42. N. Yang and K. Aoki, *The Journal of Physical Chemistry B*, 2005, **109**, 23911-23917.
43. S. S. Lee, W. Song, M. Cho, H. L. Puppala, P. Nguyen, H. Zhu, L. Segatori and V. L. Colvin, *ACS Nano*, 2013, **7**, 9693-9703.
44. R. Bali and A. T. Harris, *Industrial & Engineering Chemistry Research*, 2010, **49**, 12762-12772.

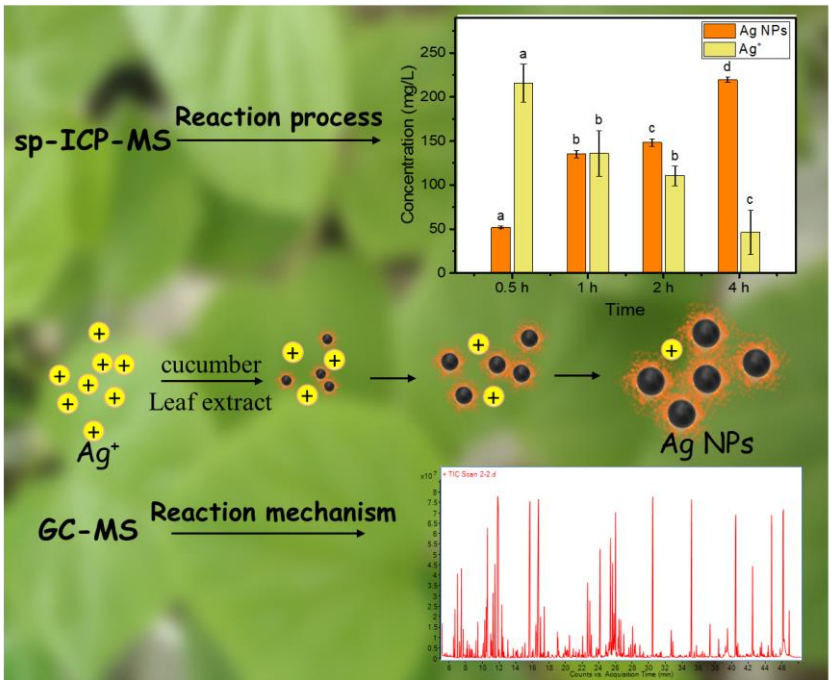

TOC